

8-2016

Scale-Dependent Linkages between Nitrate Isotopes and Denitrification in Surface Soils: Implications for Isotope Measurements and Models

Steven J. Hall

Iowa State University, stevenjh@iastate.edu

Samantha R. Weintraub

University of Utah

David Bowling

University of Utah

Follow this and additional works at: https://lib.dr.iastate.edu/eeob_ag_pubs



Part of the [Biogeochemistry Commons](#), and the [Other Ecology and Evolutionary Biology Commons](#)

The complete bibliographic information for this item can be found at https://lib.dr.iastate.edu/eeob_ag_pubs/214. For information on how to cite this item, please visit <http://lib.dr.iastate.edu/howtocite.html>.

Scale-Dependent Linkages between Nitrate Isotopes and Denitrification in Surface Soils: Implications for Isotope Measurements and Models

Abstract

Natural abundance nitrate (NO₃⁻) isotopes represent a powerful tool for assessing denitrification, yet the scale and context dependence of relationships between isotopes and denitrification have received little attention, especially in surface soils. We measured the NO₃⁻-isotope compositions in soil extractions and lysimeter water from a semi-arid meadow and lawn during snowmelt, along with the denitrification potential, bulk O₂, and a proxy for anaerobic microsites. Denitrification potential varied by three orders of magnitude and the slope of $\delta^{18}\text{O}/\delta^{15}\text{N}$ in soil-extracted NO₃⁻ from all samples measured 1.04 ± 0.12 ($R^2 = 0.64$, $p < 0.0001$), consistent with fractionation from denitrification. However, $\delta^{15}\text{N}$ of extracted NO₃⁻ was often lower than bulk soil $\delta^{15}\text{N}$ (by up to 24 ‰), indicative of fractionation during nitrification that was partially overprinted by denitrification. Mean NO₃⁻ isotopes in lysimeter water differed from soil extractions by up to 19 ‰ in $\delta^{18}\text{O}$ and 12 ‰ in $\delta^{15}\text{N}$, indicating distinct biogeochemical processing in relatively mobile water versus soil microsites. This implies that NO₃⁻ isotopes in streams, which are predominantly fed by mobile water, do not fully reflect terrestrial soil N cycling. Relationships between potential denitrification and $\delta^{15}\text{N}$ of extracted NO₃⁻ showed a strong threshold effect culminating in a null relationship at high denitrification rates. Our observations of (1) competing fractionation from nitrification and denitrification in redox-heterogeneous surface soils, (2) large NO₃⁻ isotopic differences between relatively immobile and mobile water pools, (3) and the spatial dependence of $\delta^{18}\text{O}/\delta^{15}\text{N}$ relationships suggest caution in using NO₃⁻ isotopes to infer site or watershed-scale patterns in denitrification.

Keywords

Isotope mass balance model, Mobile water, Nitrification, Redox, Snowmelt

Disciplines

Biogeochemistry | Ecology and Evolutionary Biology | Other Ecology and Evolutionary Biology

Comments

This is a manuscript of an article from *Oecologia* 181 (2016): 1221, doi: [10.1007/s00442-016-3626-1](https://doi.org/10.1007/s00442-016-3626-1). Posted with permission.

1 **Scale-dependent linkages between nitrate isotopes and denitrification in surface soils:**
2 **Implications for isotope measurements and models**

3
4 Steven J. Hall^{1,2*}, Samantha R. Weintraub^{1,3}, David R. Bowling^{1,3}

5
6 ¹Global Change and Sustainability Center, University of Utah

7 ²Department of Ecology, Evolution, and Organismal Biology, Iowa State University

8 ³Department of Geology and Geophysics, University of Utah

9 ⁴Department of Biology, University of Utah

10
11 *Contact information for corresponding author:

12 stevenjh@iastate.edu

13 608-886-6752

14 251 Bessey Hall, Iowa State University, Ames, IA 50011

15
16 *Author contributions:* SJH designed the study, SRW and DRB contributed to sample analysis and
17 interpretation, and SJH wrote the paper with contributions from SRW and DRB.

18 **Key words:** isotope mass balance model, mobile water, nitrification, redox, snowmelt

22 **Abstract**

23 Natural abundance nitrate (NO_3^-) isotopes represent a powerful tool for assessing
24 denitrification, yet the scale and context-dependence of relationships between isotopes and
25 denitrification have received little attention, especially in surface soils. We measured NO_3^-
26 isotope composition in soil extractions and lysimeter water from a semi-arid meadow and lawn
27 during snowmelt, along with denitrification potential, bulk O_2 , and a proxy for anaerobic
28 microsites. Denitrification potential varied by three orders of magnitude and the slope of
29 $\delta^{18}\text{O}/\delta^{15}\text{N}$ in soil-extracted NO_3^- from all samples measured 1.04 ± 0.12 ($R^2 = 0.64$, $p < 0.0001$),
30 consistent with fractionation from denitrification. However, $\delta^{15}\text{N}$ of extracted NO_3^- was often
31 lower than bulk soil $\delta^{15}\text{N}$ (by up to 24 ‰), indicative of fractionation during nitrification that
32 was partially overprinted by denitrification. Mean NO_3^- isotopes in lysimeter water differed from
33 soil extractions by up to 19 ‰ in $\delta^{18}\text{O}$ and 12 ‰ in $\delta^{15}\text{N}$, indicating distinct biogeochemical
34 processing in relatively mobile water vs. soil microsites. This implies that NO_3^- isotopes in
35 streams, which are predominantly fed by mobile water, do not fully reflect terrestrial soil N
36 cycling. Relationships between potential denitrification and $\delta^{15}\text{N}$ of extracted NO_3^- showed a
37 strong threshold effect culminating in a null relationship at high denitrification rates. Our
38 observations of 1) competing fractionation from nitrification and denitrification in redox-
39 heterogeneous surface soils, 2) large NO_3^- isotopic differences between relatively immobile and
40 mobile water pools, 3) and scale dependence of $\delta^{18}\text{O}/\delta^{15}\text{N}$ relationships suggest caution in using
41 NO_3^- isotopes to infer site or watershed-scale patterns in denitrification.

42

43 **Introduction**

44 Assessing gaseous nitrogen (N) losses via denitrification from soils and watersheds
45 remains a major challenge in our understanding of ecosystem N dynamics (Groffman, 2012;
46 Kulkarni et al., 2008; Yang et al., 2011). An improved understanding of the spatial and temporal
47 controls on denitrification rates, and their importance in ecosystem N budgets, is critical for
48 addressing problems linked to the cascading impacts of reactive nitrogen in our environment
49 (Galloway et al., 2003). One important method for assessing spatial and temporal patterns in
50 denitrification exploits variation in natural abundance isotopic composition ($\delta^{15}\text{N}$ and $\delta^{18}\text{O}$) of
51 nitrate (NO_3^-) and/or $\delta^{15}\text{N}$ of bulk soils to constrain denitrification losses using $\delta^{15}\text{N}$ mass
52 balance (Bai and Houlton, 2009; Houlton et al., 2006; Houlton and Bai, 2009). Recent studies
53 have expanded on this approach by combining $\delta^{15}\text{N}$ of NO_3^- with $\Delta^{17}\text{O}$, a sensitive tracer of
54 atmospheric NO_3^- (Michalski et al., 2004), to derive gross NO_3^- production (Riha et al., 2014)
55 and denitrification at the watershed scale (Fang et al., 2015). Natural abundance isotopes clearly
56 represent a powerful and minimally invasive tool to assess patterns and controls on
57 denitrification. However, several uncertainties remain with regards to the interpretation of
58 natural abundance NO_3^- isotope measurements in the context of denitrification.

59 The degree to which NO_3^- stable isotopes can record patterns of denitrification in surface
60 soil horizons (i.e., tens of cm depth), as opposed to deeper subsurface or groundwater
61 environments, has received little attention. It has long been known that significant hot-spots of
62 denitrification can occur in anaerobic microsites in otherwise aerobic soils (Parkin et al., 1987).
63 Houlton et al. (2006) found strong evidence for denitrification in wet surface soils from humid
64 tropical forests using natural abundance N isotopes. In contrast, Fang et al. (2015) used surface
65 soil NO_3^- isotope compositions as inputs to models of watershed-scale denitrification, assuming
66 that nitrification and denitrification were spatially segregated between surface and subsurface

67 soils, respectively. It remains unclear how surface soil NO_3^- samples might best be collected and
68 interpreted to inform ecosystem-scale isotope models and our broader understanding of
69 denitrification.

70 Different types of samples, such as soil salt extractions or soil water samples, could
71 differ substantially in their capacity to record NO_3^- isotope effects from denitrification due to
72 differences in water residence time and spatial distribution in the soil. Water has a continuum of
73 mobility in soil according to physical and chemical interactions with soil constituents, which can
74 be quantified according to water potential. Soil extractions capture most of the inorganic nitrogen
75 (including N interacting electrostatically with soil exchange sites) in a sampled soil volume,
76 whereas water collected in vadose zone lysimeters under minimal applied tension may reflect N
77 in comparatively mobile water pools that have a shorter residence time in the soil matrix. Water
78 pools associated with soil mineral and organic surfaces, i.e. less mobile pools, often differ greatly
79 in H_2O isotope composition relative to highly mobile water in soil macropores, reflecting
80 differences in water pool transit time and thus their capacity to record terrestrial biophysical
81 processes (Evaristo et al., 2015; Good et al., 2015). We hypothesize that these water pools might
82 also differ in their capacity to record N biogeochemical processing via stable isotopes. Both soil
83 extractions and lysimeter water collected under various tensions have been used in ecosystem-
84 scale studies involving NO_3^- isotopes, but they have seldom been directly compared. Perhaps
85 even more importantly, differences in NO_3^- stable isotopes among samples have not typically
86 been compared with canonical indices of denitrification, such as potential denitrification enzyme
87 activity.

88 Comparisons of NO_3^- isotope composition with measured potential denitrification
89 activities could help address possible ambiguities in isotope interpretation. The use of NO_3^-

90 isotopes to infer the occurrence of denitrification relies on kinetic fractionation from denitrifying
91 bacteria, which increases the $\delta^{15}\text{N}$ and $\delta^{18}\text{O}$ of residual NO_3^- (Mariotti et al., 1981). Linear
92 relationships between $\delta^{18}\text{O}$ and $\delta^{15}\text{N}$ of NO_3^- with slopes between 0.5 and 1 are assumed to
93 reflect kinetic fractionation by denitrifiers, a relationship that appears to hold across soils,
94 groundwater, and aquatic ecosystems (Cohen et al., 2012; Granger et al., 2008; Houlton et al.,
95 2006; Lehmann et al., 2003; Sigman et al., 2005). This assumption is plausible given that
96 assimilatory N fractionation by plants and microbes, another explanation for NO_3^- isotope
97 enrichment, is typically minor in N-limited ecosystems (Evans, 2001; Granger et al., 2010).
98 However, co-occurring fractionation from other N-cycling processes, such as nitrification
99 (Mariotti et al., 1981), or N inputs with differing isotope composition, could potentially obscure
100 isotope enrichment from denitrification.

101 In surface soils with heterogeneous O_2 availability, nitrification (an aerobic process) and
102 denitrification (an anaerobic process) can potentially co-occur. In open systems, nitrifying
103 bacteria tend to decrease the $\delta^{15}\text{N}$ of soil NO_3^- relative to NH_4^+ by 14 – 38 ‰ (Casciotti et al.,
104 2003; Mariotti et al., 1981). Open-system fractionation by denitrifying bacteria spans a similar
105 range, increasing $\delta^{15}\text{N}$ of the residual NO_3^- pool between 5 and 29 ‰ (Granger et al., 2008;
106 Mariotti et al., 1981). In cases where NH_4^+ or NO_3^- are fully consumed in soil microsites (i.e.,
107 closed systems), it is also possible that fractionation is partially or not at all expressed during
108 either nitrification or denitrification (Kendall et al., 2007). However, even in cases where
109 fractionation from nitrification and denitrification *are* both expressed at the microsite (ie, μm)
110 scale, it is possible that their effects could be mutually obscured over larger spatial scales (ie,
111 cm) characteristic of soil samples due to their opposite effects on $\delta^{15}\text{N}$ of NO_3^- . This situation
112 potentially creates a challenge for interpretation by obscuring the original isotope composition of

113 NO_3^- inputs, a necessary parameter for quantitative isotope models (e.g. Fang et al., 2015), and
114 diluting the pool of $\delta^{15}\text{N}$ -enriched NO_3^- that is typically used to indicate the presence of
115 denitrification (Billy et al., 2010; Houlton et al., 2006; Wexler et al., 2014). Comparing
116 traditional indices of denitrification and related biogeochemical parameters with NO_3^- isotopes
117 could help to decipher if this isotopically “cryptic” denitrification is important in surface soil
118 environments.

119 Combining measurements of $\delta^{15}\text{N}$ and $\delta^{18}\text{O}$ of NO_3^- with $\delta^{15}\text{N}$ of N sources and $\delta^{18}\text{O}$ of
120 soil water could also assist in identifying the occurrence of denitrification in surface soils. The
121 $\delta^{15}\text{N}$ of nitrified NO_3^- depends both on $\delta^{15}\text{N}$ of NH_4^+ sources and the extent of fractionation
122 during nitrification. Ammonium typically reflects the $\delta^{15}\text{N}$ of plant litter, soil organic matter
123 (SOM), or fertilizer from which it is derived, with minimal (~ 1 ‰) fractionation (Kendall et al.,
124 2007). Atmospheric deposition is another potentially important NH_4^+ source. A representative
125 range of $\delta^{15}\text{N}$ in these NH_4^+ sources that is specifically applicable to the present study is
126 indicated by the vertical shaded rectangle in Fig 1a. Nitrification of NH_4^+ fractionates $\delta^{15}\text{N}$
127 substantially in open systems (Casciotti et al., 2003; Mariotti et al., 1981), with potential values
128 indicated by the “nitrification” vertical shaded rectangle in Fig. 1a. Nitrification also imparts a
129 characteristic $\delta^{18}\text{O}$ composition to NO_3^- . Oxygen in nitrified NO_3^- is dominantly (ie, $\geq 2/3$)
130 derived from soil water, with a variable contribution from atmospheric O_2 (23.5 ‰) that depends
131 on the degree of in-situ O exchange with water (Kool et al., 2011; Mayer et al., 2001). This range
132 is indicated by the nitrification box in Fig. 1a. Subsequent denitrification of this NO_3^- pool would
133 presumably be reflected by $\sim 1:1$ increases in $\delta^{15}\text{N}$ and $\delta^{18}\text{O}$ of nitrified NO_3^- (indicated by the
134 denitrification arrow in Fig. 1a) which could ultimately return $\delta^{15}\text{N}$ of NO_3^- to values similar or

135 greater than the ecosystem N sources (Fig. 1a). However, $\delta^{18}\text{O}$ of NO_3^- would then remain
136 substantially elevated relative to $\delta^{18}\text{O}$ of soil H_2O , inconsistent with NO_3^- derived from
137 nitrification. Mixing of soil NO_3^- with atmospheric inputs is another important consideration.
138 Atmospheric NO_3^- has very high $\delta^{18}\text{O}$ (i.e., 60 – 80 ‰) as a consequence of atmospheric
139 oxidative processes (Kendall et al., 2007), which could also increase $\delta^{18}\text{O}$ of soil NO_3^- relative to
140 the products of nitrification, as indicated by the vertical mixing arrow in Fig. 1a.

141 To assess relationships between NO_3^- stable isotope composition and microsite-scale
142 denitrification in surface soils, we designed a study involving two nearby sites (a riparian
143 meadow and a managed urban lawn) in a semi-arid montane ecosystem where denitrification
144 likely represents an important fate of N during spring snowmelt. In temperate ecosystems with a
145 seasonal snowpack, snowmelt often represents a period of maximum soil moisture and potential
146 N loss, when soil biogeochemical processes are especially important in attenuating N inputs to
147 streams (Brooks and Williams, 1999; Zak et al., 1990). Our sites provided a natural gradient in
148 denitrification potential, allowing us to assess their relationship with NO_3^- isotopes while
149 maintaining similar climate and soil physical/chemical characteristics. Importantly, these sites
150 also had similar surface soil (0 – 15 cm) NH_4^+ pools, similar plant litter $\delta^{15}\text{N}$, and relatively
151 similar bulk soil $\delta^{15}\text{N}$ (within 1.5 ‰), implying that the initial $\delta^{15}\text{N}$ of NH_4^+ and NO_3^- pools
152 produced by mineralization and nitrification were also likely to be similar between sites.

153 **2. Methods**

154 We sampled soils from two sites in the Red Butte Creek watershed in Salt Lake City,
155 Utah: a natural riparian meadow with herbaceous vegetation (Dawson and Ehleringer, 1991) and
156 a managed lawn on the University of Utah campus. Both sites received $> 4 \text{ kg N ha}^{-1} \text{ y}^{-1}$ in

157 atmospheric deposition (Hall et al., in review, JGR-Biogeosciences). The lawn received ~ 100 kg
158 $\text{ha}^{-1} \text{y}^{-1}$ of fertilizer N as a urea blend (32 – 5 – 7 ratio of N, P and K) applied during late spring,
159 and ammonium sulfate (20 – 0 – 0) applied during October. Fertilizer was obtained from
160 Intermountain Farmers Association (Salt Lake City, UT). Soils were sampled following spring
161 snowmelt (Feb and Mar 2014 at the lawn and meadow, respectively), approximately five months
162 after the last fertilizer application to the lawn. Snowmelt typically represents the period of
163 maximum soil moisture in semi-arid montane ecosystems.

164 The meadow soil was a loamy Mollisol with a predominant rooting depth above 35 cm,
165 and the lawn soil was a sandy loam Inceptisol derived from local alluvium added on top of rocks.
166 Bulk density and pH were similar between sites (Table 1). We sampled the meadow at depths of
167 0 – 5, 5 – 15, and 15 – 35 cm with a 6-cm diameter auger (n = 9 for each depth); the lawn could
168 only be sampled to 15 cm due to an impenetrable rock layer (n = 12 for each depth). Tension
169 lysimeters (Prenart Super Quartz, Denmark) were installed at 15 and 35 cm in the lawn and
170 meadow, respectively, at the bottom of the main rooting zone at each site. Lysimeters were
171 installed approximately five months prior to sampling for this study. Lysimeter water was
172 sampled by applying a vacuum of -28 kPa relative to ambient pressure (86 kPa). This sampling
173 pressure was chosen because its absolute value is similar to but less than field capacity, typically
174 defined as -30 kPa for loamy soils (Schaeztl and Anderson, 2005). Field capacity is an estimate
175 of residual soil water remaining after macropores have drained. Thus, our lysimeters captured
176 water at potentials above field capacity, or a comparatively “mobile” water pool. Others have
177 used tension lysimeters to sample soil water under much more negative water potential (-70 kPa)
178 than we used here, but still judged these samples to reflect water capable of significant advection
179 (Castellano et al., 2013). We stress that the concepts of “mobile” and “immobile” water do not

180 represent a dichotomy but rather an operationally defined continuum. Because our lysimeters
181 were sampled under tension, they contain some fraction of soil-associated water differing in
182 composition from water that instantaneously drains through soils during melt or precipitation
183 events (Landon et al., 1999). Our operational separation between more and less mobile water
184 pools, respectively sampled in lysimeters and soil extractions, is thus conservative. Water
185 samples were collected throughout the period of snowmelt (total n = 186; Jan – April 2014).

186 Oxygen (O₂) sensors (Apogee Instruments, Logan, Utah) were installed at depths of 10
187 cm in 4.8 cm diameter polyvinylchloride pipes with sealed caps (equilibration chambers), where
188 the bottom lip of the chamber was pressed into undisturbed soil (Hall et al., 2013). Soil O₂
189 content was recorded on a datalogger at 15-minute intervals. Here, we report O₂ during the
190 period of NO₃⁻ sample collection. All of the above measurements were made in the context of a
191 snow removal experiment at each site (Hall et al., 2016a), but given the absence of treatment
192 effects on any biogeochemical response variable, we do not report treatment identities for ease of
193 interpretation. Precipitation was collected on an event basis during the study period for analysis
194 of NO₃⁻ and NH₄⁺ concentrations and isotope composition. Lysimeter and precipitation samples
195 were filtered through pre-combusted and rinsed Whatman GF/F filters and frozen until analysis
196 by ion chromatography.

197 We measured potential denitrification rates in shaken slurries of soil samples within 24
198 hours of sampling using the acetylene inhibition method (Groffman et al., 1999), using an
199 incubation temperature of 4 °C to approximate field conditions and 25 °C to facilitate
200 comparisons with other studies. Potential denitrification rates are an appropriate metric to
201 compare with the isotope composition of NO₃⁻ pools because they are tightly linked to the
202 abundance of bacterial denitrification functional genes, which integrate recent process activity in

203 the soil environment (Petersen et al., 2012). Soil subsamples were extracted in 2M potassium
204 chloride (KCl) solutions for analysis of NH_4^+ and NO_3^- concentrations and isotope composition.
205 We measured $\delta^{15}\text{N}$ and $\delta^{18}\text{O}$ of NO_3^- in soil extractions ($n = 50$), lysimeter water samples ($n =$
206 31), and precipitation samples ($n = 8$) using *Pseudomonas aureofaciens* and the denitrifier
207 method (Bell and Sickman, 2014; Casciotti et al., 2002) to generate N_2O for analysis by isotope
208 ratio mass spectrometry at the Stable Isotope Ratio Facility for Environmental Research at the
209 University of Utah. When analyzing the soil extractions using the denitrifier method, we
210 corrected for the presence of trace NO_3^- in KCl and any physiological effects on the denitrifying
211 bacteria by analyzing reference materials prepared in the same matrix (Bell and Sickman, 2014).
212 Samples were normalized to δ notation, relative to atmospheric N_2 for N and VSMOW for O,
213 using a combination of the international NO_3^- reference materials USGS 34, 35 and 32. Precision
214 and accuracy were 0.6 ‰ and 0.7 ‰ (respectively) for $\delta^{15}\text{N}$, and 0.6 ‰ and 0.3 ‰ (respectively)
215 for $\delta^{18}\text{O}$, assessed by repeated analysis of IAEANO3 (for $\delta^{15}\text{N}$) and USGS 32 (for $\delta^{18}\text{O}$) treated
216 as unknowns. Sample reproducibility was 0.3 ‰, based on duplicate analyses of 1/8 of the
217 samples. To characterize $\delta^{15}\text{N}$ of fertilizer inputs to the lawn, three subsamples were analyzed
218 from each of two production batches of each fertilizer type (ammonium sulfate and urea). Bulk
219 soil $\delta^{15}\text{N}$ from each site and sampled depth increment, and surface litter ($n = 9$ plots per site),
220 were analyzed on samples dried at 60 °C. Soil and fertilizer $\delta^{15}\text{N}$ were measured via combustion
221 on an elemental analyzer coupled to an isotope ratio mass spectrometer (Thermo MAT 253,
222 Waltham MA). A subset of lysimeter water samples from the meadow site ($n = 17$) was analyzed
223 for $\delta^{18}\text{O}$ of H_2O by isotope ratio infrared spectroscopy (Picarro L-2130i, Santa Clara CA).

224 A subset of precipitation samples ($n = 15$) was analyzed for $\delta^{15}\text{N}$ of NH_4^+ using a
225 modified NH_3 diffusion method (Holmes et al., 1998). Briefly, 30 ml of sample was added to a

226 60 ml HDPE bottle with 1.5 g sodium chloride. A glass-fiber filter acidified with 30 μ l of 4M
227 phosphoric acid was pressed between Teflon tape and added to the bottle. Magnesium oxide (90
228 mg) was added to volatilize NH_3 , and the bottle was immediately capped and incubated for 7
229 days on an orbital shaker/incubator at 40 °C to allow NH_3 to be completely trapped as NH_4^+ on
230 the acidified filter. Filters were analyzed for $\delta^{15}\text{N}$ (precision < 0.2‰) by combustion as described
231 above. Analysis of ammonium sulfate solutions with known $\delta^{15}\text{N}$ values verified a lack of
232 fractionation during diffusion.

233 Soil subsamples were also extracted in the field immediately after sampling with 0.5 M
234 hydrochloric acid for analysis of reduced and oxidized iron (Fe(II) and Fe(III), respectively) as a
235 redox indicator (Hall et al., 2013). The presence of Fe(II) implies the presence of anaerobic
236 microsites where dissimilatory Fe reduction exceeds Fe(II) oxidation by O_2 . The ratio of
237 Fe(II)/Fe_{HCl} reflects the proportion of HCl-extractable Fe that has been reduced, facilitating
238 comparisons among sites that may differ in total HCl-extractable Fe content (Hall et al., 2015).
239 Thermodynamic principles imply that NO_3^- should have been consumed via denitrification in
240 microsites where Fe(II) is present (Chapelle et al., 1995).

241 We analyzed linear relationships between $\delta^{15}\text{N}$ and $\delta^{18}\text{O}$ of NO_3^- both within and among
242 sites and for each separate sample type (soil extractions vs. lysimeter water) using ANCOVA.
243 Mean differences in $\delta^{15}\text{N}$ and $\delta^{18}\text{O}$ composition among sites were assessed using MANOVA (ie,
244 ANOVA testing two response variables simultaneously). Differences in other response variables
245 among sites were assessed with ANOVA. Relationships between $\delta^{15}\text{N}$ of NO_3^- and potential
246 denitrification and Fe(II)/Fe_{HCl} were highly non-linear, so we fit trends with a two-component
247 piecewise linear regression using the SiZer package in R (Sonderegger 2012).

248 **Results**

249 While both sites typically had near-atmospheric O₂ concentrations in the bulk soil
250 throughout the period of measurement, they also showed evidence of redox heterogeneity and the
251 presence of reducing conditions in soil microsites as reflected by Fe(II)/Fe_{HCl} ratios (Table 1).
252 The lawn had much higher Fe(II)/Fe_{HCl} relative to the meadow ($p < 0.0001$), coinciding with
253 increased potential denitrification rates. Denitrification potential was 16-fold greater in lawn
254 soils at 4 °C ($p < 0.0001$) and 6-fold greater at 25 °C ($p < 0.001$; Table 1) when considering all
255 depth increments combined. Nitrate concentrations in soil extractions were generally similar
256 between sites, although lysimeter NO₃⁻ was significantly greater in the lawn (Table 1).

257 Bulk soil δ¹⁵N was similar between sites in 0 – 5 cm soil, but was slightly (1.5 ‰) and
258 significantly ($p < 0.0001$) greater in lawn 5 – 15 cm soil (Table 1). Despite the fact that NH₄⁺
259 concentrations significantly differed between sites at a given depth increment ($p < 0.001$), total
260 KCl extractable NH₄⁺ mass to 15 cm was similar between the meadow and lawn, measuring
261 0.056 (0.013) and 0.044 (0.003) kg NH₄⁺-N ha⁻¹, respectively. At the lawn, comparison of the
262 KCl extractable NH₄⁺ pool with annual NH₄⁺ fertilizer inputs indicated that > 99.9 % of the
263 previous year fertilizer application was assimilated, or otherwise transformed or exported, prior
264 to measurement. Surface litter δ¹⁵N was also similar between the meadow (-0.5 ± 0.1 ‰) and
265 lawn (0.1 ± 0.4 ‰). Fertilizer δ¹⁵N was highly consistent within and between production batches
266 and was relatively similar between the two fertilizer types applied here. Two separate batches of
267 ammonium sulfate δ¹⁵N measured -0.9 ± 0.2 and -1.0 ± 0.3 ‰, and the urea blend δ¹⁵N was -1.7
268 ± 0.1 and -1.6 ± 0.3 ‰. Values of δ¹⁵N of NH₄⁺ in bulk atmospheric deposition measured $-1.2 \pm$
269 1.5 ‰, similar to fertilizer.

270 Trends in $\delta^{18}\text{O}$ and $\delta^{15}\text{N}$ of NO_3^- in soil extractions from both sites considered together
271 were consistent with linear isotopic effects from denitrification of NO_3^- sources with similar
272 initial isotope values, reflected by a slope of 1.04 ± 0.12 ($R^2 = 0.64$, $p < 0.0001$; Fig. 1b). The
273 slope of this relationship did not differ significantly between sites. However, the relationship
274 between $\delta^{18}\text{O}$ and $\delta^{15}\text{N}$ was insignificant when assessing samples from the lawn alone (slope =
275 0.62 , $R^2 = 0.10$, $p = 0.21$) and was much stronger in the meadow (slope = 0.72 ± 0.13 , $p < 0.0001$,
276 $R^2 = 0.55$). Nevertheless, the lawn extractions had significantly greater (more enriched) NO_3^-
277 $\delta^{18}\text{O}$ and $\delta^{15}\text{N}$ values than the meadow ($p < 0.0001$; Fig. 1b, Table 2). Nitrate $\delta^{15}\text{N}$ in soil
278 extractions also had a weakly significant site by depth interaction ($p = 0.02$), where values did
279 not differ by depth in the lawn but were significantly greater in meadow 0 – 5 cm samples than
280 the deeper samples.

281 In contrast to the soil extractions, $\delta^{18}\text{O}$ and $\delta^{15}\text{N}$ of lysimeter NO_3^- were not significantly
282 correlated, and lysimeter NO_3^- isotope composition did not differ between sites (Fig. 1b, Table 2).
283 Furthermore, lysimeter samples significantly differed in NO_3^- isotope composition when
284 compared with soil extractions from the same site (MANOVA, $p < 0.0001$; Fig. 1b). Values of
285 $\delta^{18}\text{O}$ in precipitation NO_3^- (81.9 ± 4.0 ‰) were substantially greater than any of the soil
286 extractions or soil lysimeter samples, while $\delta^{15}\text{N}$ of precipitation NO_3^- (2.3 ± 0.7 ‰; Table 2) fell
287 within the bounds of soil extractions and lysimeter samples. Neither the soil extractions nor
288 lysimeter samples displayed significant relationships between NO_3^- isotope composition and
289 NO_3^- concentrations (data not shown).

290 Nitrate $\delta^{15}\text{N}$ showed distinct trends with potential denitrification and $\text{Fe(II)/Fe}_{\text{HCl}}$ at both
291 sites: significant linear trends at the meadow ($p < 0.001$ and 0.03 , respectively), but no

292 relationship at the lawn. Combined, these data suggested significant threshold relationships
293 between $\delta^{15}\text{N}$, potential denitrification, and $\text{Fe(II)}/\text{Fe}_{\text{HCl}}$ as determined by piecewise linear
294 regressions (Fig. 2). Nitrate $\delta^{15}\text{N}$ initially increased sharply with potential denitrification (slope =
295 0.75, between 0.10 and 0.90 with 95 % confidence) and $\text{Fe(II)}/\text{Fe}_{\text{HCl}}$ (slope = 170, between 60
296 and 550 with 95 % confidence), but subsequently plateaued to slopes indistinguishable from zero
297 for both response variables (Fig. 2).

298 **Discussion**

299 We found evidence that denitrification was likely occurring during snowmelt in surface
300 soil horizons at both sites, as reflected by substantial rates of potential denitrification activity
301 combined with the presence of anaerobic microsites as reflected by $\text{Fe(II)}/\text{Fe}_{\text{HCl}}$. Although high
302 potential denitrification rates indicate the presence of denitrifying organisms, they do not
303 definitively indicate when denitrification may have occurred. In these ecosystems, increased soil
304 moisture during snowmelt likely generated anaerobic microsites that promoted denitrification,
305 given that very low soil moisture (< 10 % by volume) prevailed for several months prior at each
306 site until snowmelt began (Hall et al., 2016a). The importance of denitrification in cold soils
307 during snowmelt has been well established in other studies (Brooks et al., 2011), and our
308 measured potential denitrification activities at 25 °C were similar to rates from wetland and
309 riparian soils in other studies (Roach and Grimm, 2011). Yet, different NO_3^- samples (soil
310 extractions vs. lysimeter water) and sites (the lawn and meadow) varied dramatically in their
311 relationships between $\delta^{15}\text{N}$ and $\delta^{18}\text{O}$ and proxies for denitrification.

312 *Trends in NO_3^- isotopes in soil extractions and proxies for denitrification*

313 Plotting $\delta^{18}\text{O}$ vs. $\delta^{15}\text{N}$ of NO_3^- in soil extractions from both sites yielded a slope similar
314 to one, consistent with the upper bound of slopes invoked as evidence for denitrification in
315 previous field studies in terrestrial, groundwater, and marine environments (Cohen et al., 2012;
316 Houlton et al., 2006; Lehmann et al., 2003; Sigman et al., 2005), and similar to laboratory
317 experiments with denitrifying bacteria (Granger et al., 2008). However, $\delta^{15}\text{N}$ of NO_3^- remained
318 lower than bulk soil N in most samples, despite the fact that denitrification had demonstrably
319 occurred. These trends are consistent with a large initial isotope fractionation from nitrification
320 (Casciotti et al., 2003) which was subsequently impacted by denitrification to a variable extent
321 among samples. A large fractionation from nitrification is consistent with the observed presence
322 of excess NH_4^+ at both sites relative to NO_3^- (Table 1), and comparatively slow enzymatic
323 catalysis in cold soils following snowmelt. A large isotopic effect of nitrification was also
324 recently observed in New Zealand pasture soils during winter (Wells et al., 2015).

325 Our interpretations of $\delta^{15}\text{N}$ of NO_3^- are enhanced by considering potential variation in
326 $\delta^{15}\text{N}$ of the NH_4^+ from which NO_3^- is derived. We argue that there were not likely to be
327 systematic differences in $\delta^{15}\text{N}$ of NH_4^+ between sites, according to the following reasoning. The
328 major potential sources of NH_4^+ at these sites during the period of sampling include
329 mineralization of litter and SOM, residual fertilizer at the lawn, and atmospheric deposition.
330 Most importantly for our study, these potential NH_4^+ sources had relatively similar $\delta^{15}\text{N}$
331 composition in comparison with the observed variation in $\delta^{15}\text{N}$ of NO_3^- , and tended to be similar
332 between sites. First, mineralized NH_4^+ has similar $\delta^{15}\text{N}$ (± 1 ‰) relative to the organic matter
333 (e.g., litter or SOM) from which it was derived (Kendall et al., 2007), and differences in litter
334 and SOM $\delta^{15}\text{N}$ pools between the two sites were small (< 0.5 and 1.5 ‰, respectively). Multiple
335 litter and SOM pools mineralize NH_4^+ at different rates, so it is likely that the measured

336 differences between litter and bulk soil $\delta^{15}\text{N}$ (-0.5 to 5.8 ‰) approximate the range of variation
337 in $\delta^{15}\text{N}$ of mineralized NH_4^+ at these sites. Mean fertilizer (-0.9 – 0.1 ‰) and atmospheric
338 deposition (2.3 ‰) $\delta^{15}\text{N}$ fell close to or within this range. We suggest that mineralization of litter
339 and SOM (as opposed to fertilizer) were especially important sources of NH_4^+ in both the
340 meadow and the lawn during the period of sampling. This interpretation was supported by 1) the
341 fact that total extractable NH_4^+ stocks were *equivalent* between lawn and meadow despite
342 fertilization; 2) the very small extractable pool of NH_4^+ relative to annual fertilizer inputs,
343 indicative of rapid cycling of mineral N where > 99.9 % of fertilizer N inputs were assimilated or
344 lost via gaseous or leaching pathways prior to sampling; 3) the fact that six months had elapsed
345 since fertilizer application, providing ample opportunity for assimilation or other transformations.
346 Even if residual fertilizer did represent a significant component of soil NH_4^+ , it is unlikely to lead
347 to substantial differences in $\delta^{15}\text{N}$ of NH_4^+ between sites given that fertilizer $\delta^{15}\text{N}$ was very
348 similar to litter $\delta^{15}\text{N}$ at both sites.

349 Secondly, it is plausible to assume that initial $\delta^{15}\text{N}$ values of nitrified NO_3^- may also have
350 been similar between sites and depths. This assumption is reasonable given overall similarities in
351 NH_4^+ concentrations, bulk soil N concentration and $\delta^{15}\text{N}$, microbial biomass N, pH, bulk density,
352 and climate between the lawn and meadow (Hall et al., 2016a). Under this assumption, the lawn
353 showed greater enrichment of $\delta^{15}\text{N}$ and $\delta^{18}\text{O}$ subsequent to nitrification, implying a greater
354 fraction of NO_3^- loss to denitrification relative to the meadow in agreement with the
355 denitrification potential assays. Trends in $\delta^{15}\text{N}$ of NO_3^- with depth in the lawn also corresponded
356 with the denitrification potential assays: $\delta^{15}\text{N}$ of NO_3^- was greater in 0 – 5 cm soils, which had
357 greater potential denitrification rates. Previous studies have similarly demonstrated greater

358 denitrification potential in surface than subsurface soil horizons (Groffman et al., 2002) and have
359 reported high denitrification rates in lawns (Raciti et al., 2011). Both factors reflect the
360 importance of plant C and N inputs (and potentially fertilizer additions) as controls on
361 denitrification in surface soils, as opposed to O₂ diffusion limitation in the subsurface. However,
362 if we had assessed relationships between $\delta^{18}\text{O}$ and $\delta^{15}\text{N}$ of NO_3^- at the lawn site alone without
363 the context of the meadow samples with much lower denitrification rates, this conclusion would
364 have been obscured. The meadow samples revealed the likely importance of fractionation during
365 nitrification, and without accounting for this fractionation we would have had little isotopic
366 evidence for denitrification at the lawn—even though denitrification potential assays and Fe(II)
367 measurements strongly suggested it had occurred. This highlights a critical limitation in the use
368 of NO_3^- isotopes to infer site-specific or watershed-scale patterns of denitrification, as recently
369 implemented elsewhere.

370 *Contrasting NO_3^- isotope compositions in soil extractions and lysimeter water*

371 In contrast to the linear trend in the soil extractions, $\delta^{18}\text{O}$ and $\delta^{15}\text{N}$ values in soil
372 lysimeter NO_3^- exhibited significant scatter, likely reflecting multiple fractionating processes and
373 mixing with atmospheric NO_3^- that was enriched in ^{18}O . The NO_3^- isotope disparities between
374 lysimeters and soil extractions may also reflect the redox heterogeneity of terrestrial soils
375 (Sexstone et al., 1985). Measurements of Fe(II)/Fe_{HCl} in soil extractions suggested the presence
376 of reducing conditions in soil microsites, whereas the soil O₂ sensors indicated highly aerobic
377 conditions at the scale of the bulk soil atmosphere in both sites (Table 1). Differences in dual
378 isotope ($\delta^{18}\text{O}/\delta^{15}\text{N}$) slopes and $\delta^{15}\text{N}$ and $\delta^{18}\text{O}$ values between the soil extractions and the
379 lysimeters support our hypothesis that soil extractions and lysimeter samples differ in their
380 capacity to record ecosystem-scale N biogeochemical cycling via stable isotopes. A plausible

381 explanation for this pattern is that soil extractions sampled the anaerobic microsites inside soil
382 aggregates where denitrification can occur (Parkin et al., 1987), whereas lysimeters largely
383 reflected the transport of N that was nitrified in the aerobic macropore environment or in surface
384 litter.

385 This distinction may be critical in interpreting patterns of denitrification at the watershed
386 scale, where the NO_3^- isotopic composition of stream water is often assumed to integrate gross
387 nitrification or denitrification across entire watersheds (Fang et al., 2015; Riha et al., 2014). Our
388 data suggest that this assumption does not necessarily hold, given that relatively mobile lysimeter
389 water and soil extractions from the same sites differed substantially in their NO_3^- isotope
390 composition. Rather, as supported by recent syntheses of H_2O isotope dynamics, these samples
391 may reflect two “water worlds”: poorly mobile water accessible to plants and microbes, and
392 comparatively mobile water that dominates groundwater recharge and stream discharge (Evaristo
393 et al., 2015; Good et al., 2015). Thus, stream or groundwater NO_3^- isotope composition may not
394 necessarily reflect denitrification in surface soil microsites, a dominant zone of potential
395 denitrification activity due to elevated inputs of C and N (Groffman et al., 2002).

396 *Implications for interpreting $\delta^{15}\text{N}$ in models and environmental samples*

397 Importantly, dual isotope trends in soil KCl extractable NO_3^- from both sites combined
398 were consistent with denitrification isotope effects (Fig. 1) and were related to potential
399 denitrification rates (Fig. 2) despite the fact that $\delta^{15}\text{N}$ values of NO_3^- were typically less than
400 bulk soil $\delta^{15}\text{N}$. This finding has interesting implications for models that estimate denitrification
401 at the ecosystem scale using isotopic measurements of NO_3^- (Billy et al., 2010; Fang et al., 2015).
402 Our data suggest that substantial denitrification might occur even in situations where $\delta^{15}\text{N}$ values

403 of NO_3^- do not display substantial enrichment relative to N inputs or other ecosystem pools, due
404 to the potentially large initial N isotope fractionation associated with nitrification. Thus, isotope
405 models which assume that $\delta^{15}\text{N}$ of surface soil NO_3^- predominantly represents the product of
406 nitrification (Fang et al., 2015) would tend to underestimate the relative importance of
407 denitrification in the case where large fractionation effects of nitrification were partially
408 counteracted by denitrification. In the latter study (ibid.), correlations between $\delta^{15}\text{N}$ and $\delta^{18}\text{O}$ of
409 NO_3^- were not significant in surface soil KCl extractions, leading the authors to conclude that
410 NO_3^- dynamics were spatially separated in these sites, with nitrification dominating in near-
411 surface soils and denitrification prevailing in deeper soils.

412 The very weak linear trends between $\delta^{15}\text{N}$ and $\delta^{18}\text{O}$ we observed at the lawn site alone
413 (as opposed to considering all samples together), combined with our process-level measurements,
414 show that denitrification is not necessarily well recorded by site-specific trends in NO_3^- isotope
415 composition in surface soils. Rather, $\delta^{15}\text{N}$ of NO_3^- showed a threshold relationship with potential
416 denitrification rates and reducing conditions—strong trends at low rates that became a null
417 relationship at higher rates. This may reflect closed-system kinetics where NO_3^- is mostly
418 consumed via denitrification in soil microsites, leading to an under-expression of kinetic isotope
419 effects as noted previously in both soils and sediments (Houlton et al., 2006; Sebilo et al., 2003).
420 Thus, pairwise trends between $\delta^{15}\text{N}$ and $\delta^{18}\text{O}$ of NO_3^- and their relationships with potential
421 denitrification only became strongly significant when considering a very broad gradient in redox
422 variability and potential denitrification activity (which spanned three orders of magnitude among
423 samples and sites, Figure 2). Moreover, our results are consistent with a recent global-scale
424 analysis of soil $\delta^{15}\text{N}$, which found that much of the variability in bulk soil $\delta^{15}\text{N}$ previously
425 attributed to denitrification might instead be explained by clay content and preferential retention

426 of microbially-processed organic matter (Craine et al., 2015). Differences in clay content
427 between our sites (with loam and sandy loam texture, respectively) could contribute to the fact
428 that bulk soil $\delta^{15}\text{N}$ did not reflect the large site differences in denitrification potential and $\delta^{15}\text{N}$ of
429 soil extracted NO_3^- .

430 In summary, recent analytical and conceptual advances related to NO_3^- isotopes provide
431 powerful opportunities for exploring controls on N sources and biogeochemical processing over
432 multiple spatial scales (Fang et al., 2015; Houlton et al., 2006; Kendall et al., 2007; Michalski et
433 al., 2004; Riha et al., 2014). We showed that surface soils characterized by denitrification at the
434 microsite scale in a heterogeneous redox environment can exhibit NO_3^- isotope trends consistent
435 with denitrification when examining samples exhibiting a broad range of potential denitrification
436 rates. However, these patterns are highly dependent on spatial scale (i.e., comparisons among vs.
437 within sites), sample type (soil extractions vs. lysimeter water), and assumptions about NH_4^+
438 isotope composition, nitrification isotope effects, and initial NO_3^- isotope composition prior to
439 any denitrification. Thus, we suggest that NO_3^- isotope data should be interpreted with careful
440 consideration of boundary conditions, sample types, and hydrologic connectivity between
441 sampled pools before using them as parameter inputs or response variables in N cycling models.

442 **Acknowledgements**

443 We gratefully acknowledge field and lab assistance from Simone Jackson, Jillian Turner,
444 Dave Eiriksson, Kendalynn Morris, and contributions from Suvankar Chakraborty, Gabe Bowen,
445 and Jim Ehleringer in implementing the denitrifier method at SIRFER. This research was
446 supported by NSF EPSCoR grant IIA 1208732 awarded to Utah State University, as part of the
447 State of Utah Research Infrastructure Improvement Award, and by NSF grant DBI-1337947.

448 Any opinions, findings, and conclusions or recommendations expressed are those of the author(s)
449 and do not necessarily reflect the views of the National Science Foundation.

450 **References**

451 Bai, E., Houlton, B.Z., 2009. Coupled isotopic and process-based modeling of gaseous nitrogen
452 losses from tropical rain forests. *Global Biogeochemical Cycles* 23, GB2011.

453 doi:10.1029/2008GB003361

454 Bell, M.D., Sickman, J.O., 2014. Correcting for background nitrate contamination in KCl-
455 extracted samples during isotopic analysis of oxygen and nitrogen by the denitrifier
456 method. *Rapid Communications in Mass Spectrometry* 28, 520–526.

457 doi:10.1002/rcm.6824

458 Billy, C., Billen, G., Sebilo, M., Birgand, F., Tournebize, J., 2010. Nitrogen isotopic composition
459 of leached nitrate and soil organic matter as an indicator of denitrification in a sloping
460 drained agricultural plot and adjacent uncultivated riparian buffer strips. *Soil Biology and*
461 *Biochemistry* 42, 108–117. doi:10.1016/j.soilbio.2009.09.026

462 Brooks, P.D., Grogan, P., Templer, P.H., Groffman, P., Öquist, M.G., Schimel, J., 2011. Carbon
463 and nitrogen cycling in snow-covered environments. *Geography Compass* 5, 682–699.

464 doi:10.1111/j.1749-8198.2011.00420.x

465 Brooks, P.D., Williams, M.W., 1999. Snowpack controls on nitrogen cycling and export in
466 seasonally snow-covered catchments. *Hydrological Processes* 13, 2177–2190.

467 doi:10.1002/(SICI)1099-1085(199910)13:14/15<2177::AID-HYP850>3.0.CO;2-V

468 Casciotti, K.L., Sigman, D.M., Hastings, M.G., Böhlke, J.K., Hilkert, A., 2002. Measurement of
469 the oxygen isotopic composition of nitrate in seawater and freshwater using the denitrifier

470 method. *Analytical Chemistry* 74, 4905–4912. doi:10.1021/ac020113w

471 Casciotti, K.L., Sigman, D.M., Ward, B.B., 2003. Linking diversity and stable isotope
472 fractionation in ammonia-oxidizing bacteria. *Geomicrobiology Journal* 20, 335–353.

473 Castellano, M.J., Lewis, D.B., Kaye, J.P., 2013. Response of soil nitrogen retention to the
474 interactive effects of soil texture, hydrology, and organic matter. *Journal of Geophysical*
475 *Research: Biogeosciences* 118, 280–290. doi:10.1002/jgrg.20015

476 Chapelle, F.H., McMahon, P.B., Dubrovsky, N.M., Fujii, R.F., Oaksford, E.T., Vroblesky, D.A.,
477 1995. Deducing the distribution of terminal electron-accepting processes in
478 hydrologically diverse groundwater systems. *Water Resources Research* 31, 359–371.

479 Cohen, M.J., Heffernan, J.B., Albertin, A., Martin, J.B., 2012. Inference of riverine nitrogen
480 processing from longitudinal and diel variation in dual nitrate isotopes. *Journal of*
481 *Geophysical Research: Biogeosciences* 117, G01021. doi:10.1029/2011JG001715

482 Craine, J.M., Elmore, A.J., Wang, L., Augusto, L., Baisden, W.T., Brookshire, E.N.J., Cramer,
483 M.D., Hasselquist, N.J., Hobbie, E.A., Kahmen, A., Koba, K., Kranabetter, J.M., Mack,
484 M.C., Marin-Spiotta, E., Mayor, J.R., McLauchlan, K.K., Michelsen, A., Nardoto, G.B.,
485 Oliveira, R.S., Perakis, S.S., Peri, P.L., Quesada, C.A., Richter, A., Schipper, L.A.,
486 Stevenson, B.A., Turner, B.L., Viani, R.A.G., Wanek, W., Zeller, B., 2015. Convergence
487 of soil nitrogen isotopes across global climate gradients. *Scientific Reports* 5, 8280.
488 doi:10.1038/srep08280

489 Dawson, T.E., Ehleringer, J.R., 1991. Streamside trees that do not use stream water. *Nature* 350,
490 335–337. doi:10.1038/350335a0

491 Evans, R.D., 2001. Physiological mechanisms influencing plant nitrogen isotope composition.
492 *Trends in Plant Science* 6, 121–126. doi:10.1016/S1360-1385(01)01889-1

493 Evaristo, J., Jasechko, S., McDonnell, J.J., 2015. Global separation of plant transpiration from
494 groundwater and streamflow. *Nature* 525, 91–94. doi:10.1038/nature14983

495 Fang, Y., Koba, K., Makabe, A., Takahashi, C., Zhu, W., Hayashi, T., Hokari, A.A., Urakawa,
496 R., Bai, E., Houlton, B.Z., Xi, D., Zhang, S., Matsushita, K., Tu, Y., Liu, D., Zhu, F.,
497 Wang, Z., Zhou, G., Chen, D., Makita, T., Toda, H., Liu, X., Chen, Q., Zhang, D., Li, Y.,
498 Yoh, M., 2015. Microbial denitrification dominates nitrate losses from forest ecosystems.
499 *Proceedings of the National Academy of Sciences* 112, 1470–1474.
500 doi:10.1073/pnas.1416776112

501 Galloway, J.N., Aber, J.D., Erisman, J.W., Seitzinger, S.P., Howarth, R.W., Cowling, E.B.,
502 Cosby, B.J., 2003. The nitrogen cascade. *BioScience* 53, 341–356. doi:10.1641/0006-
503 3568(2003)053[0341:TNC]2.0.CO;2

504 Good, S.P., Noone, D., Bowen, G., 2015. Hydrologic connectivity constrains partitioning of
505 global terrestrial water fluxes. *Science* 349, 175–177. doi:10.1126/science.aaa5931

506 Granger, J., Sigman, D.M., Lehmann, M.F., Tortell, P.D., 2008. Nitrogen and oxygen isotope
507 fractionation during dissimilatory nitrate reduction by denitrifying bacteria. *Limnology
508 and Oceanography* 53, 2533–2545.

509 Granger, J., Sigman, D.M., Rohde, M.M., Maldonado, M.T., Tortell, P.D., 2010. N and O
510 isotope effects during nitrate assimilation by unicellular prokaryotic and eukaryotic
511 plankton cultures. *Geochimica et Cosmochimica Acta* 74, 1030–1040.
512 doi:10.1016/j.gca.2009.10.044

513 Groffman, P.M., 2012. Terrestrial denitrification: challenges and opportunities. *Ecological
514 Processes* 1, 1–11.

515 Groffman, P.M., Boulware, N.J., Zipperer, W.C., Pouyat, R.V., Band, L.E., Colosimo, M.F.,
516 2002. Soil nitrogen cycle processes in urban riparian zones. *Environmental Science &*
517 *Technology* 36, 4547–4552. doi:10.1021/es020649z

518 Groffman, P.M., Holland, E.A., Myrold, D.D., Robertson, G.P., Zou, X., 1999. Denitrification,
519 in: Robertson, G.P., Bledsoe, C.S., Coleman, D.C., Sollins, P. (Eds.), *Standard Soil*
520 *Methods for Long-Term Ecological Research*. Oxford University Press, New York, pp.
521 272–290.

522 Hall, S.J., McDowell, W.H., Silver, W.L., 2013. When wet gets wetter: Decoupling of moisture,
523 redox biogeochemistry, and greenhouse gas fluxes in a humid tropical forest soil.
524 *Ecosystems* 16, 576–589. doi:10.1007/s10021-012-9631-2

525 Hall S.J., Silver W.L. (2015) Reducing conditions, reactive metals, and their interactions can
526 explain spatial patterns of surface soil carbon in a humid tropical forest. *Biogeochemistry*
527 125:149–165. doi: 10.1007/s10533-015-0120-5

528 Hall, S.J., Weintraub, S.R., Eiriksson, D., Brooks, P.D., Baker, M.A., Bowen, G.J., Bowling,
529 D.R., 2016a. Stream nitrogen inputs reflect groundwater across a snowmelt-dominated
530 montane to urban watershed. *Environmental Science & Technology* 50, 1137–1146.
531 doi:10.1021/acs.est.5b04805

532 Hall, S.J., Baker, M.A., Jones, S.B., Stark, J., Bowling, D.R., 2016b. Contrasting soil nitrogen
533 dynamics across a montane meadow and urban lawn in a semi-arid watershed. *Urban*
534 *Ecosystems* In press. doi:10.1007/s11252-016-0538-0

535 Holmes, R.M., McClelland, J.W., Sigman, D.M., Fry, B., Peterson, B.J., 1998. Measuring ^{15}N -
536 NH_4^+ in marine, estuarine and fresh waters: An adaptation of the ammonia diffusion

537 method for samples with low ammonium concentrations. *Marine Chemistry* 60, 235–243.
538 doi:10.1016/S0304-4203(97)00099-6

539 Houlton, B.Z., Bai, E., 2009. Imprint of denitrifying bacteria on the global terrestrial biosphere.
540 *Proceedings of the National Academy of Sciences* 106, 21713–21716.
541 doi:10.1073/pnas.0912111106

542 Houlton, B.Z., Sigman, D.M., Hedin, L.O., 2006. Isotopic evidence for large gaseous nitrogen
543 losses from tropical rainforests. *Proceedings of the National Academy of Sciences* 103,
544 8745–8750. doi:10.1073/pnas.0510185103

545 Kendall, C., Elliott, E.M., Wankel, S.D., 2007. Tracing anthropogenic inputs of nitrogen to
546 ecosystems, in: Michener, R., Lajtha, K. (Eds.), *Stable Isotopes in Ecology and*
547 *Environmental Science*. Blackwell Publishing Ltd, pp. 375–449.

548 Kool, D.M., Wrage, N., Oenema, O., Van Kessel, C., Van Groenigen, J.W., 2011. Oxygen
549 exchange with water alters the oxygen isotopic signature of nitrate in soil ecosystems.
550 *Soil Biology and Biochemistry* 43, 1180–1185. doi:10.1016/j.soilbio.2011.02.006

551 Kulkarni, M.V., Groffman, P.M., Yavitt, J.B., 2008. Solving the global nitrogen problem: it's a
552 gas! *Frontiers in Ecology and the Environment* 6, 199–206. doi:10.1890/060163

553 Landon, M.K., Delin, G.N., Komor, S.C., Regan, C.P., 1999. Comparison of the stable-isotopic
554 composition of soil water collected from suction lysimeters, wick samplers, and cores in
555 a sandy unsaturated zone. *Journal of Hydrology* 224, 45–54. doi:10.1016/S0022-
556 1694(99)00120-1

557 Lehmann, M.F., Reichert, P., Bernasconi, S.M., Barbieri, A., McKenzie, J.A., 2003. Modelling
558 nitrogen and oxygen isotope fractionation during denitrification in a lacustrine redox-

559 transition zone. *Geochimica et Cosmochimica Acta* 67, 2529–2542. doi:10.1016/S0016-
560 7037(03)00085-1

561 Mariotti, A., Germon, J.C., Hubert, P., Kaiser, P., Letolle, R., Tardieux, A., Tardieux, P., 1981.
562 Experimental determination of nitrogen kinetic isotope fractionation: Some principles;
563 illustration for the denitrification and nitrification processes. *Plant and Soil* 62, 413–430.
564 doi:10.1007/BF02374138

565 Mayer, B., Bollwerk, S.M., Mansfeldt, T., Hütter, B., Veizer, J., 2001. The oxygen isotope
566 composition of nitrate generated by nitrification in acid forest floors. *Geochimica et*
567 *Cosmochimica Acta* 65, 2743–2756. doi:10.1016/S0016-7037(01)00612-3

568 Michalski, G., Meixner, T., Fenn, M., Hernandez, L., Sirulnik, A., Allen, E., Thiemens, M., 2004.
569 Tracing atmospheric nitrate deposition in a complex semiarid ecosystem using $\Delta^{17}\text{O}$.
570 *Environmental Science & Technology* 38, 2175–2181. doi:10.1021/es034980+

571 Parkin, T., Starr, J., Meisinger, J., 1987. Influence of sample size on measurement of soil
572 denitrification. *Soil Science Society of America Journal* 51, 1492–1501.

573 Petersen, D.G., Blazewicz, S.J., Firestone, M., Herman, D.J., Turetsky, M., Waldrop, M., 2012.
574 Abundance of microbial genes associated with nitrogen cycling as indices of
575 biogeochemical process rates across a vegetation gradient in Alaska. *Environmental*
576 *Microbiology* 14, 993–1008. doi:10.1111/j.1462-2920.2011.02679.x

577 Raciti, S.M., Burgin, A.J., Groffman, P.M., Lewis, D.N., Fahey, T.J., 2011. Denitrification in
578 suburban lawn soils. *Journal of Environment Quality* 40, 1932. doi:10.2134/jeq2011.0107

579 Riha, K.M., Michalski, G., Gallo, E.L., Lohse, K.A., Brooks, P.D., Meixner, T., 2014. High
580 atmospheric nitrate inputs and nitrogen turnover in semi-arid urban catchments.
581 *Ecosystems* 17, 1309–1325. doi:10.1007/s10021-014-9797-x

582 Roach, W.J., Grimm, N.B., 2011. Denitrification mitigates N flux through the stream–floodplain
583 complex of a desert city. *Ecological Applications* 21, 2618–2636. doi:10.1890/10-1613.1

584 Schaetzl, R.J., Anderson, S., 2005. *Soils: Genesis and Geomorphology*. Cambridge University
585 Press.

586 Sebilo, M., Billen, G., Grably, M., Mariotti, A., 2003. Isotopic composition of nitrate-nitrogen as
587 a marker of riparian and benthic denitrification at the scale of the whole Seine River
588 system. *Biogeochemistry* 63, 35–51. doi:10.1023/A:1023362923881

589 Sexstone, A., Revsbech, N., Parkin, T., Tiedje, J., 1985. Direct measurement of oxygen profiles
590 and denitrification rates in soil aggregates. *Soil Science Society of America Journal* 49,
591 645–651.

592 Sigman, D.M., Granger, J., DiFiore, P.J., Lehmann, M.M., Ho, R., Cane, G., van Geen, A., 2005.
593 Coupled nitrogen and oxygen isotope measurements of nitrate along the eastern North
594 Pacific margin. *Global Biogeochemical Cycles* 19, GB4022. doi:10.1029/2005GB002458

595 Wells, N.S., Baisden, W.T., Clough, T.J., 2015. Ammonia volatilisation is not the dominant
596 factor in determining the soil nitrate isotopic composition of pasture systems. *Agriculture,
597 Ecosystems & Environment* 199, 290–300. doi:10.1016/j.agee.2014.10.001

598 Wexler, S.K., Goodale, C.L., McGuire, K.J., Bailey, S.W., Groffman, P.M., 2014. Isotopic
599 signals of summer denitrification in a northern hardwood forested catchment.
600 *Proceedings of the National Academy of Sciences* 111, 16413–16418.
601 doi:10.1073/pnas.1404321111

602 Yang, W.H., Teh, Y.A., Silver, W.L., 2011. A test of a field-based ¹⁵N–nitrous oxide pool
603 dilution technique to measure gross N₂O production in soil. *Global Change Biology* 17,
604 3577–3588. doi:10.1111/j.1365-2486.2011.02481.x

605 Zak, D.R., Groffman, P.M., Pregitzer, K.S., Christensen, S., Tiedje, J.M., 1990. The vernal dam:
606 plant-microbe competition for nitrogen in northern hardwood forests. *Ecology* 71, 651–
607 656. doi:10.2307/1940319
608

Table 1: Soil biogeochemical characteristics by depth for the lawn and meadow sites. Standard errors are in parentheses.

Site	Depth	pH	Bulk density (g cm ⁻³)	Soil δ ¹⁵ N	Soil N (%)	Soil N stock (kg N ha ⁻¹)	Fe(II) (μg g ⁻¹)	Fe(II)/ Fe _{HCl}	KCl- extractable NH ₄ ⁺ (μg g ⁻¹)	KCl- extractable NO ₃ ⁻ (μg g ⁻¹)	Lysimeter NO ₃ ⁻ -N (mg l ⁻¹)	Potential denitrification (μg N ₂ O-N g ⁻¹ h ⁻¹ at 25 °C)	Potential denitrification (μg N ₂ O-N g ⁻¹ h ⁻¹ at 4 °C)	Bulk soil O ₂ (%)
Lawn	0 - 5	7.5 (0.1)	0.86 (0.02)	3.3 (0.3)	0.36 (0.02)	1500 (200)	53 (7)	0.46 (0.08)	8.8 (1.5)	4.4 (1.8)	--	2955 (194)	406 (55)	--
	5 - 15	7.8 (0.1)	--	5.8 (0.1)	0.12 (0.01)	1800 (300)	23 (1)	0.32 (0.08)	2.1 (0.3)	1.3 (0.5)	0.67 (0.23)	709 (40)	35 (3)	19.6 (1.1)
Meadow	0 - 5	7.7 (0.1)	0.87 (0.02)	3.8 (0.1)	0.41 (0.02)	1800 (200)	7 (1)	0.04 (0.01)	2.4 (0.2)	2.5 (0.2)	--	465 (62)	25 (3)	--
	5 - 15	7.7 (0.1)	--	4.3 (0.1)	0.36 (0.01)	3100 (300)	8 (1)	0.03 (0)	3.9 (0.3)	2.9 (0.2)	--	217 (20)	11 (3)	20.7 (0.1)
	15 - 35	7.8 (0.1)	--	5.5 (0.1)	0.23 (0.01)	4000 (400)	7 (1)	0.03 (0)	3.6 (0.3)	1.1 (0.1)	0.24 (0.04)	65 (15)	3 (0)	--

Table 2: Nitrate isotope composition in soil KCl extractions and lysimeter samples from the lawn and meadow. Water $\delta^{18}\text{O}$ values from meadow lysimeters are also presented; these were very similar to precipitation $\delta^{18}\text{O}$ during the period of sampling (Hall et al., 2016b). Values in parentheses represent standard errors.

Site	Sample type	Sample size	$\text{NO}_3^- \delta^{15}\text{N}$ (‰)	$\text{NO}_3^- \delta^{18}\text{O}$ (‰)
Lawn	Lysimeter (NO_3^-)	15	-1.2 (1.7)	-9.5 (1.2)
Lawn	Soil extract (NO_3^-)	23	4.2 (1.2)	9.6 (2.4)
Meadow	Lysimeter (NO_3^-)	16	1.7 (0.5)	-12.5 (3.2)
Meadow	Soil extract (NO_3^-)	27	-9.9 (1.2)	-8.4 (1.2)
Meadow	Lysimeter (H_2O)	17	--	-17.7 (0.4)
Salt Lake City	Precipitation NO_3^-	8	2.3 (0.7)	81.9 (4.0)

Figure captions

Figure 1: a) Conceptual dual isotope plot ($\delta^{18}\text{O}$ and $\delta^{15}\text{N}$) showing measured variation of $\delta^{15}\text{N}$ of SOM, litter, and fertilizer as a vertical rectangle and measured variation of precipitation $\delta^{18}\text{O}$ as a horizontal rectangle. The predicted isotope composition of nitrified NO_3^- with complete expression of kinetic isotope effects on $\delta^{15}\text{N}$ is bounded by a black rectangle. This incorporates potential N fractionation during nitrification of an NH_4^+ source with $\delta^{15}\text{N}$ within the observed range of SOM, litter, and fertilizer, and $\text{NO}_3^- \delta^{18}\text{O}$ ranging from complete incorporation of soil water to a 1/3 contribution from atmospheric O_2 with $\delta^{18}\text{O} = 23.5$ ‰ (Kool et al., 2011; Mayer et al., 2001). The dotted line represents an illustrative trend of kinetic denitrification isotope effects with a $\delta^{18}\text{O}/\delta^{15}\text{N}$ slope of one, beginning at an arbitrary point in $\delta^{18}\text{O}/\delta^{15}\text{N}$ space. The vertical arrow indicates potential impacts of mixing with atmospheric NO_3^- enriched in $\delta^{18}\text{O}$. b)

Measurements of NO_3^- isotopes in soil KCl extractions (black symbols) and lysimeter water samples (open symbols). Triangles and circles represent the lawn and meadow sites, respectively. The dashed line represents a linear regression of $\delta^{18}\text{O}$ and $\delta^{15}\text{N}$ values in soil KCl extractions from both sites (slope = 1.04 ± 0.12 , $R^2 = 0.64$, $p < 0.0001$).

Figure 2: a) Relationship between $\delta^{15}\text{N}$ of NO_3^- in soil extractions and potential denitrification rate; the grey line represents a piecewise linear regression as described in the text. b)

Relationships between $\delta^{15}\text{N}$ of NO_3^- in soil extractions and the $\text{Fe(II)}/\text{Fe}_{\text{HCl}}$ ratio (a redox indicator, described in the text and Hall et al., 2015); the grey line represents a piecewise linear regression.

Figure 1:

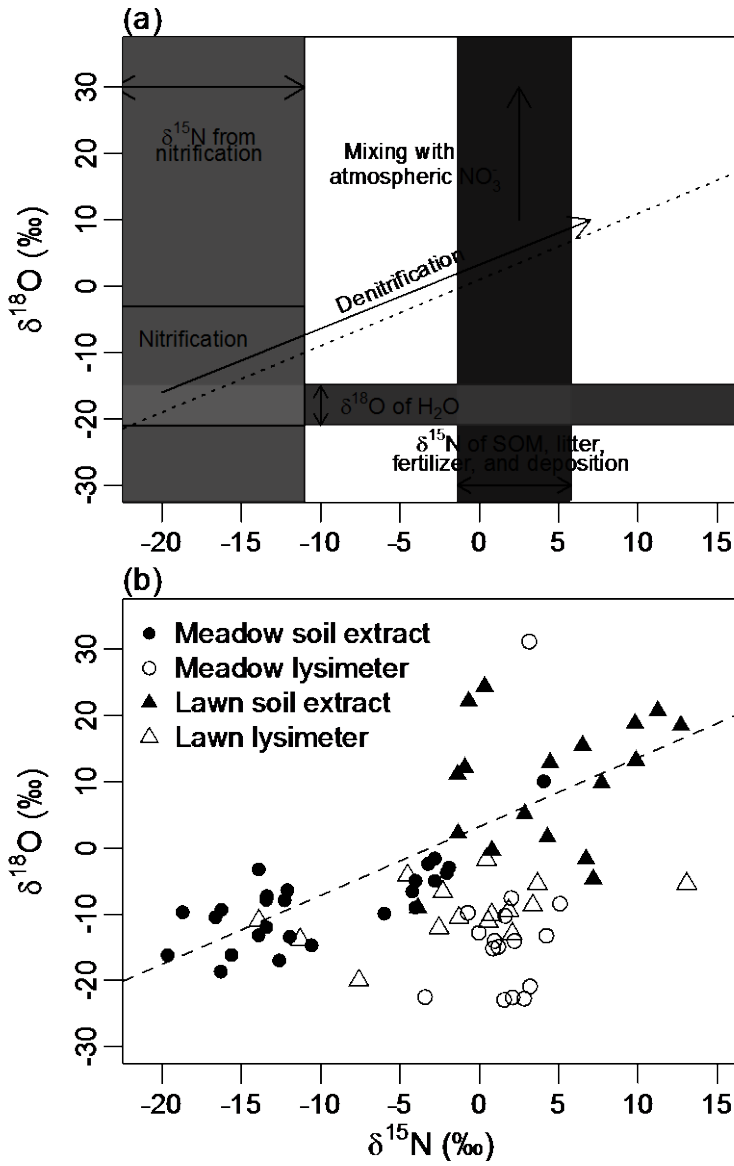


Figure 2:

